

# 基于 Fourier 拟合曲面的 X 射线焊缝缺陷检测

李雪琴<sup>1</sup>, 刘培勇<sup>2</sup>, 殷国富<sup>2</sup>, 蒋红海<sup>3</sup>

(1. 西华大学 机械工程与自动化学院, 成都 610039; 2. 四川大学 制造科学与工程学院, 成都 610065;  
3. 昆明理工大学 机电工程学院, 昆明 650504)

**摘 要:** 针对在强噪声、低对比度及复杂背景特征下 X 射线焊缝图像的缺陷检测问题, 提出了去噪处理、焊缝边缘分割及缺陷检测的方法. 用快速离散 Curvelet 变换和循环平移相结合的方法, 对焊缝图像进行滤波去噪, 同时对图像列灰度曲线用最大类间方差法提取焊缝区域. 在图像预处理后, 采用三阶 Fourier 曲线对图像列灰度曲线进行拟合并扩展到三维空间, 构造出自适应阈值面, 最后利用原图像与构造曲面三维灰度图的灰度值差异, 准确分割背景与缺陷区域. 结果表明, 与传统缺陷检测算法相比, 该方法能准确提取出焊缝缺陷, 漏检率和误判率低, 准确率可达 95%.

**关键词:** X 射线; 焊缝图像; 缺陷检测; Curvelet 变换; Fourier 拟合

**中图分类号:** TG 115.28   **文献标识码:** A   **文章编号:** 0253-360X(2014)10-0061-04

## 0 序 言

在焊接过程中, 由于各种因素影响, 导致焊缝中含有裂纹、气孔、夹杂、未熔合、未焊透等缺陷, 直接影响焊接结构件的质量和寿命, 因此焊缝缺陷检测十分重要. 目前焊接件质量检测广泛应用 X 射线无损检测技术. X 射线焊缝图像具有噪声多、对比度低、存在较大的背景起伏等特点<sup>[1]</sup>, 因此缺陷检测的准确性、实时性、适应性一直是焊缝图像缺陷检测的主要问题.

国内外学者对 X 射线焊缝图像的缺陷自动检测进行了探索和研究, 并提出了很多方法: 孙怡等人<sup>[2]</sup>提出一种基于空间对比度与空间方差的模糊识别算法检测焊缝缺陷, 该方法对气孔、夹杂等圆形缺陷有较好的检测效果, 但应用范围较窄. 梁珊等人<sup>[3]</sup>利用 B 样条曲线平滑优化焊缝列灰度值, 提取极值集合, 分析确定出焊缝缺陷边界并提取, 该方法克服了焊缝复杂纹理对缺陷提取的影响, 但对对比度非常低的微弱缺陷检测效果不佳. Wang 等人<sup>[4]</sup>采用基于多阈值和支持向量机的裂纹缺陷检测方法. Lim 等人<sup>[5]</sup>采用人工神经网络对焊缝缺陷分类, 都能较好的提取缺陷, 但它们算法复杂, 计算量大, 通常不能满足在线实时测量的要求.

结合以上方法的优缺点, 文中提出了针对 X 射

线焊缝图像去噪及缺陷分割提取的新算法模型, 并通过试验验证了该算法在噪声多、对比度低的焊缝图像中能准确提取出缺陷, 为焊缝缺陷自动检测系统提供了理论依据.

## 1 图像分析

在 X 射线焊缝图像的获取和传输过程中, 由于各种因素的影响, 图像中会生成大量噪声, 影响图像质量, 加上图像信号弱、信噪比低、对比度差、清晰度低等特点, 影响了对被检测构件进行分析和评价的效果. 为了提高图像呈现效果, 便于后续算法处理分析, 必须采取适当的方法对图像进行去噪处理. 目前, 一般采用空域或频域处理法去除图像噪声. 对焊缝图像本身而言可能存在各种缺陷, 所以在去噪的同时要尽量保留这些细节信息, 曲波变换具有很好地表达图像边缘和细节的特点, 适合焊缝图像去噪.

### 1.1 基于快速离散 Curvelet 变换的图像去噪

#### 1.1.1 Curvelet 变换

1999 年第一代曲波 (Curvelet) 变换理论被提出, 但是, 它的数字实现过程较复杂且会带来巨大的数据冗余度, 因此, Candès 等人<sup>[6]</sup>提出了更简单、更便于理解的快速离散曲波变换算法 (fast discrete curvelet transform, FDCT), 即第二代曲波变换.

笛卡尔坐标系下, 图像  $f[t_1, t_2]$  ( $0 \leq t_1, t_2 < n$ ) 为输入, 离散 Curvelet 变换的曲波系数可定义为

$$c^D(j, l, k) = \sum_{0 \leq t_1, t_2 < n} f[t_1, t_2] \overline{\varphi_{j, l, k}^D[t_1, t_2]} \quad (1)$$

式中:  $\overline{\varphi_{j, l, k}^D[t_1, t_2]}$  为数字 Curvelet 波形函数取值的平均值;  $j, l, k$  分别表示尺度、方向、位置参量。

第二代 Curvelet 变换有两种数值实现方法, 一种是基于非均匀采样的快速 Fourier 变换; 另一种是基于特殊选择的 Fourier 采样的卷绕<sup>[7]</sup>。文中采用基于特殊选择的 Fourier 采样的卷绕和循环平移(cycle spinning)<sup>[8]</sup>相结合方法进行焊缝去噪。

### 1.1.2 基于 FDCT 的图像去噪算法

曲波变换中较大的曲波系数对应较强的边缘, 噪声对应较小的系数。因此, 在阈值选取上, 要保留较大系数、舍弃较小系数以实现图像去噪。虽然用阈值法能降噪的同时保留图像的局部特征, 但由于曲波变换不具有平移不变性, 图像边缘处会出现“振铃”效应, 即产生伪吉布斯现象。为了抑制阈值去噪过程中由于缺乏不变性而产生的伪吉布斯现象, 采

用循环平移方法平移图像来改变不连续点的位置。

算法的处理步骤如下。

(1) 对噪声图像  $f_n$  做循环平移(平移范围取 1)。

(2) 对平移后的图像进行基于卷绕的曲波变换, 得到各尺度、各方向的曲波系数  $c^D(j, l, k)$ 。

(3) 通过蒙特卡洛分析方法估计噪声方差, 在最细尺度上取阈值系数 2.5, 其它各个尺度上取阈值系数 2.2, 阈值处理后的曲波系数为  $\hat{c}^D(j, l, k)$ 。

(4) 对  $\hat{c}^D(j, l, k)$  进行逆曲波变换和逆循环平移。

(5) 重复步骤(2)~步骤(4), 对迭代后的结果求平均值, 得到最终去噪后图像  $f$ 。

为了验证该算法去噪的优越性, 选取  $512 \times 64$  像素大小的焊缝图像为实例进行试验。

图 1 是焊缝图像在噪声标准偏差  $\sigma = 5$  用中值滤波、均值滤波、小波去噪及文中算法的去噪效果比较图。

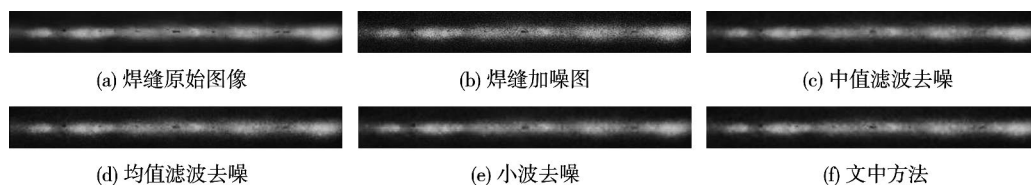


图 1 加噪图像各去噪方法结果比较

Fig. 1 Comparison of de-noising via different approaches

表 1 是焊缝图像加不同标准偏差的白噪声后, 各种去噪图像的峰值信噪比的比较。

表 1 焊缝图像去噪前后的峰值信噪比(dB)

Table 1 PSNR of weld image before and after filtering

	噪声标准差 $\delta$			
	5	10	15	20
去噪前	91.1396	85.122 4	81.623 8	79.162 9
中值滤波	98.666	94.292 1	91.480 8	89.275 4
均值滤波	97.266 2	93.598 5	90.661 1	88.472 1
小波去噪	99.602 1	95.982 5	92.994 1	90.680 4
文中算法	100.007 8	96.098 8	93.152	90.926 7

可以看到, 与其它方法相比, 文中去噪算法更好地去除了焊缝图像的噪声, 保持了图像的边缘和细节信息, 去噪后的峰值信噪比有明显提高, 去噪结果更接近原图。

### 1.2 边界分割提取焊缝区域

在 X 射线焊缝图像中, 为了能够消除无效数据对检测造成的干扰, 提取焊缝区域是非常必要的。鉴于焊缝图像整体灰度分布不均, 文中对焊缝图像

每列灰度曲线应用最大类间方差(Otsu)法确定焊缝区域, 该方法是在图像灰度直方图的基础上用最小二乘法原理推导出来的, 它以目标和背景类间方差最大或类内方差最小为阈值选取准则, 具有良好的分割效果。提取图 1a 去噪后的焊缝区域并二值化处理, 结果如图 2 所示。



图 2 焊缝区域二值化图像

Fig. 2 Binarization image of weld region

## 2 Fourier 曲线拟合提取缺陷

### 2.1 Fourier 曲线

曲线拟合是用平滑曲线拟合多个离散点, 是数据分析最常见的方法之一, 它是尽可能接近离散数据点但不是全部通过。Fourier 级数逼近是曲线拟合的常用方法。

Fourier 级数拟合基本模型为

$$f(x) = a_0 + \sum_{n=1}^{\infty} (a_n \cos n\omega x + b_n \sin n\omega x) \quad (2)$$

式中:  $a_0$  为常数;  $a_n \cos n\omega x + b_n \sin n\omega x$  为  $n$  阶谐波;  $\omega = 2\pi/T$ ,  $T$  为周期.

### 2.2 拟合列灰度曲线

对图像进行垂直于焊缝的线扫描, 取焊缝图像第 328 列与第 425 列像素点的灰度值, 如图 3 所示. 图 3a 为含圆柱和条状缺陷的基于 FDCT 去噪的焊缝图像, 图 3b 为 X 射线焊缝图像第 328 列无缺陷扫描线的灰度像素值拟合曲线, 图 3c 为第 425 列有缺陷扫描线的灰度像素值拟合曲线. 其中实线是基于全部像素点的拟合, 虚线采用 Fourier 三阶拟合. 可以看出, 没有缺陷的焊缝图像两条拟合曲线几乎重合, 而有缺陷的焊缝图像在缺陷位置原始列灰度拟合曲线值远小于 Fourier 三阶拟合曲线值.

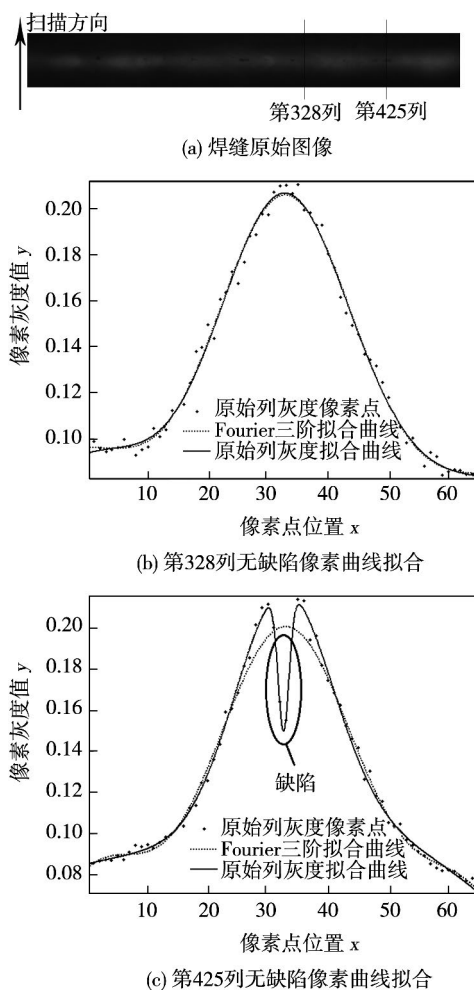


图 3 列扫描焊缝图像曲线拟合结果  
Fig. 3 Curve-fitting result of weld image

### 2.3 构造阈值面提取缺陷

基于以上分析, 提取焊缝图像缺陷的算法如下.

(1) 采用 FDCT\_WARP 和 Cycle Spinning 相结

合的方法对原始焊缝图像  $f(i, j)$  进行去噪处理, 得去噪图像  $f_n(i, j)$ .

(2) 对图像  $f_n(i, j)$  进行垂直于焊缝方向的线扫描, 对扫描线进行 Fourier 三阶拟合, 得一系列拟合曲线  $N(j)$ , 其中  $j=1, 2, \dots, i$ .

(3) 将二维列拟合曲线  $N(j)$  合成扩展到三维空间, 得到基于列扫描自适应阈值曲面  $S(i, j)$ .

(4) 比较去噪图像  $f_n(i, j)$  与 Fourier 拟合曲面  $S(i, j)$  各点灰度像素值大小, 得到焊缝缺陷图像的二值图  $f_d(i, j)$ , 即

$$f_d(i, j) = \begin{cases} 1 & f_n(i, j) < S(i, j) + c \\ 0 & f_n(i, j) > S(i, j) + c \end{cases} \quad (3)$$

式中:  $c$  为常系数, 一般取  $0.015 \sim 0.035$ .

(5) 用 Otsu 法分割提取焊缝边界区域并二值化处理得图像  $f_r(i, j)$ , 将图像  $f_r(i, j)$  和  $f_d(i, j)$  做与运算, 得修正后的焊缝缺陷图像.

运用文中算法进行 Fourier 三阶曲线拟合的自适应阈值面的灰度三维图如图 4 所示, 图 5 为焊缝缺陷最终检测结果.

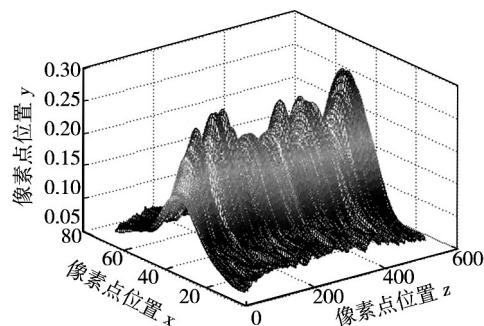


图 4 Fourier 拟合阈值面灰度三维图

Fig. 4 3-D gray image of Fourier fitting threshold surface



图 5 缺陷检测结果

Fig. 5 Defects extraction result

为了验证文中算法的优越性, 对原始缺陷图像直接用 Otsu 算法进行检测, 结果如图 6 所示. 可以看出, 用 Otsu 算法不能准确提取焊缝缺陷, 容易产生低对比度缺陷漏检的情况.



图 6 Otsu 算法检测结果

Fig. 6 Result of Otsu method

### 3 焊缝缺陷提取试验及结果

为了验证文中方法的有效性,选取了 100 幅 X 射线焊缝图像在 matlab 仿真平台进行试验,其中包括 60 幅缺陷图像和 40 幅合格图像. 对于缺陷焊缝,共检测出 58 条,错误接受率 =  $(60 - 58) / 60 = 3.33\%$ ,没能检测出缺陷的主要原因是由于部分紧邻焊缝边缘微小缺陷被误判为焊缝边缘;对于合格焊缝,共检测出 38 条,正确拒绝率 =  $(40 - 38) / 40 = 5\%$ ;准确率 =  $(58 + 38) / 100 = 96\%$ ,达到了较好的检测效果.

取其中有代表性的图像缺陷检测结果,如图 7 所示. 可以看出,各类焊接缺陷如裂纹、夹渣未焊透等都可以被成功检测出,失真小,鲁棒性强.

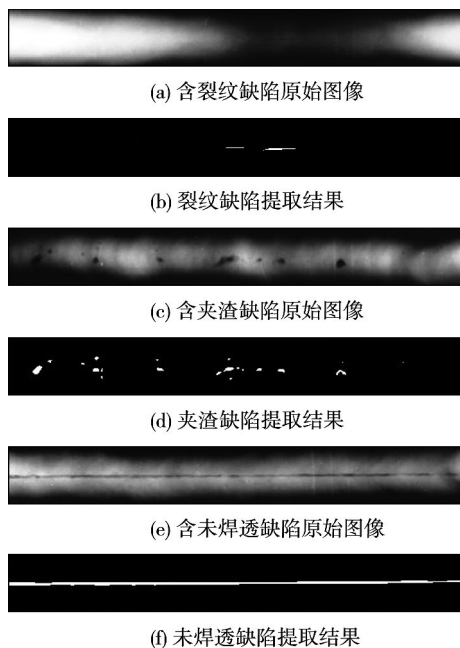


图 7 各种缺陷提取结果

Fig. 7 Various defects extraction result

### 4 结 论

(1) 采用基于特殊选择的 Fourier 采样的卷绕和循环平移相结合的方法,有效的去除了焊缝噪声,明显提高了图像峰值信噪比,保持了缺陷原貌,失真小.

(2) 用最大类间方差法确定焊缝区域,防止产生焊缝边缘外的伪缺陷.

(3) 基于三阶 Fourier 方程对列灰度曲线进行拟合处理,构造自适应阈值面,利用阈值面与原图像的三维灰度图的灰度值差异,有效提取出焊缝缺陷.

(4) 试验对比验证了文中方法适用于各种类型和大小的缺陷,针对背景复杂、噪声大、对比度低的图像有很好的分割效果,准确性高.

#### 参考文献:

- [1] 邵家鑫,都东,朱新杰,等. 基于 X 射线数字化图像处理的双面焊缝缺陷检测[J]. 焊接学报,2010,31(11): 21-24. Shao Jiaxin, Du Dong, Zhu Xinjie, et al. Weld defect detection of double sides weld based on X-ray digitized image [J]. Transactions of the China Welding Institution, 2010, 31(11): 21-24.
- [2] 孙怡,孙洪雨,白鹏,等. X 射线焊缝图像中缺陷的实时检测方法[J]. 焊接学报,2004,25(2): 115-118. Sun Yi, Sun Hongyu, Bai Peng, et al. Real-time automatic detection of weld defects in X-ray images [J]. Transactions of the China Welding Institution, 2004, 25(2): 115-118.
- [3] 梁 珊,魏艳红,占小红. 基于 B 样条曲线的 X 射线图像焊缝缺陷分割与提取[J]. 焊接学报,2012,33(7): 109-112. Liang Peng, Wei Yanhong, Zhan Xiaohong. Weld defect segmentation and extraction of X-ray image based on B-spline curve [J]. Transactions of the China Welding Institution, 2012, 33(7): 109-112.
- [4] Wang Y, Sun Y, Lü P, et al. Detection of line weld defects based on multiple thresholds and support vector machine [J]. Nondestructive Testing and Evaluation International, 2008, 41: 517-524.
- [5] Lim T Y, Ratnam M M, Khalid M A. Automatic classification of weld defects using simulated data and an MLP neural network [J]. Insight, 2007, 49(3): 154-159.
- [6] Candès E J, Donoho D L. New tight frames of curvelets and optimal representations of objects with piecewise C2 singularities [J]. Communication on Pure and Applied Mathematics, 2004, 57(2): 219-266.
- [7] Candès E, Demanet L, Donoho D, et al. Fast discrete curvelet transforms [J]. Multiscale Modeling and Simulation, 2006, 5(3): 861-899.
- [8] Coifman R R, Donoho D L. Translation-invariant de-noising [C]// Wavelets and Statistics, Lecture Notes in Statistics. New York: Springer-Verlag, 1995: 125-150.

作者简介: 李雪琴,女,1986 年出生,博士. 主要从事图像处理、机器视觉系统方面的研究. 发表论文 4 篇. Email: 6326935@qq.com

通讯作者: 殷国富,男,博士,教授,博士研究生导师. Email: gfyin@scu.edu.cn

**Microstructure and wear resistance of laser amorphous-nanocrystals reinforced Ni-based coating on TA15 titanium alloy** LI Jianing<sup>1,2</sup>, GONG Shuili<sup>1</sup>, LI Huaixue<sup>1</sup>, SHAN Feihu<sup>1</sup> (1. Science and Technology on Power Beam Processes Laboratory, Beijing Aeronautical Manufacturing Technology Research Institute, Beijing 100024, China; 2. Aviation Industry Corporation of China, Beijing Institute of Aeronautical Materials, Beijing 100095, China). pp 57 – 60

**Abstract:** Coaxial powder feeding laser cladding of the Ni60A-Ni coated WC-TiB<sub>2</sub>-Y<sub>2</sub>O<sub>3</sub> mixed powders on the aviation material TA15 titanium alloy substrate can form an amorphous-nanocrystals reinforced composite coating. Such coating was researched by means of the microstructure observation, the micro-hardness test and the dry friction and wear test at room temperature. Investigation indicated that the such coating mainly consisted of  $\gamma$ -(Fe, Ni), WC,  $\alpha$ -W<sub>2</sub>C, M<sub>12</sub>C, Ti-B compounds, Ti-Al intermetallics, amorphous phases and the Mo, Zr, V carbides. Amorphous, nanocrystalline and the other crystalline phases were existence in such coating. This coating also exhibited a better wear resistance than TA15 titanium alloy, and abrasive grain wear mechanism and the adhere wear mechanism did the process at the same time during the dry sliding wear process. The productions of the nanocrystals made the worn surface more smooth, favoring the decrease of the coefficient of friction and the wear volume losses.

**Key words:** laser cladding; surface modifications; wear properties

**Weld defect detection by X-ray images method based on Fourier fitting surface** LI Xueqin<sup>1</sup>, LIU Peiyong<sup>2</sup>, YIN Guofu<sup>2</sup>, JIANG Honghai<sup>3</sup> (1. School of Mechanical Engineering and Automation, Xihua University, Chengdu 610039, China; 2. School of Manufacturing Science and Engineering, Sichuan University, Chengdu 610065, China; 3. School of Electrical and Mechanical Engineering, Kunming University of Science and Technology, Kunming 650504, China). pp 61 – 64

**Abstract:** To solve such problems as the strong noise, low contrast and complex background of X-ray image in the weld defect detection, a method of the noise reduction, weld edge segmentation and defects extraction was proposed. The fast discrete curvelet transform and cycle shift were applied to reduce noise of the weld image, and the Otsu method was utilized to extract the weld region by the column gray curves of the image. Cubic Fourier curve was used to fit the column gray curves after preprocessing of weld image, and the adaptive threshold surface was constructed by extending fitting curves to 3D space. Finally, the background and the defect area were segmented accurately with the gray differences of 3D gray image between the original image and the reconstructed surface. Experiment results show that the method can extract weld defects accurately. Compared with traditional defect detection algorithm, it has the lower undetected rate and fewer misinterpretations, the accuracy rate could reach 95%.

**Key words:** X-ray; weld image; defect detection; curvelet transform; Fourier fitting

**Effects of laser scanning welding process on porosity rate of aluminum alloy** ZHOU Litao, WANG Wei, WANG Xuyou, WANG Shiyang, SUN Qian (Harbin Welding Institute, China

Academy of Machinery Science and Technology, Harbin 150028, China). pp 65 – 68, 72

**Abstract:** Research of 6061 aluminum alloy was done by using laser-scanning welding. The effects of such scanning parameters as track, width and frequency on porosity tendency were studied. The result showed that laser-scanning welding with the path of vertical, parallel and circular to welds can reduce the porosity of aluminum alloy compared with laser welding without scanning and the circular pattern was the best. The scanning width and scanning frequency of laser also have important influence on porosity, which can be controlled within 0.5% as the scanning width was greater than 0.65 mm and scanning frequency was from 100 to 220 Hz. The producing of porosity was associated with weld shape and the lower of depth-to-width ratio of the weld can help to control the porosity.

**Key words:** aluminum alloy; laser scanning welding; porosity inhibition

**Corrosion behavior of weld joints of substation grounding grid** FENG Lajun<sup>1</sup>, DENG Bo<sup>1</sup>, YAN Aijun<sup>2</sup>, ZHANG Jing<sup>1</sup> (1. Material Corrosion and Protection Key Laboratory of Xi'an, Xi'an University of Technology, Xi'an 710048, China; 2. Shaanxi Electric Power Research Institute, Xi'an 710054, China). pp 69 – 72

**Abstract:** To provide foundation for corrosion protection of the weld metal using in grounding grid, the corrosion difference between the weld and base metal of grounding grid was studied by electrochemical noise and field coupon method. The results showed that there were many transients in the time series of the weld of Q235 steel for grounding grid in soil of Shaanxi Xiaoyi substation, while a few transients in the time series of the Q235 base metal, which indicated that weld corrosion was more sensitive to discharge voltage of grounding grid. The noise resistance of the weld metal,  $R_n$ , was  $3.38 \times 10^4 \Omega/\text{cm}^2$  during the corrosion process, and the  $R_n$  of the weld was  $1.44 \times 10^4 \Omega/\text{cm}^2$ . The corrosion rate of the weld metal was 0.067 mm/a, and for the welded joint was 0.077 mm/a. The based metal was in a uniform type of corrosion and the weld was mainly in a pitting type of corrosion.

**Key words:** grounding grid; weld corrosion; electrochemical noise; localized corrosion

**Research on toughness weak points of joints of NiCrMoV refractory steel for manufacturing steam turbine rotor** LI Yifei<sup>1</sup>, CAI Zhipeng<sup>1</sup>, PAN Jiluan<sup>1</sup>, LIU Xia<sup>1,2</sup>, WANG Peng<sup>2</sup>, HUO Xin<sup>2</sup>, SHEN Hongwei<sup>2</sup> (1. Department of Mechanical Engineering, Tsinghua University, Beijing 100084, China; 2. Shanghai Electric Power Generation Equipment Co. Ltd., Shanghai 200240, China). pp 73 – 76, 80

**Abstract:** The toughness weak points of multi-layer and multi-pass weld of 30Cr2Ni4MoV refractory steel steam turbine welded rotor were studied by means of simulated heat welded layers with the emphasis on the forming of the toughness weak points and its influence on the toughness. The methods of optical microscope analysis, scanning electron microscopy analysis and transmission electron microscope analysis were utilized. The experimental results show that there are many M-A constituents in the carbon-rich areas of welded layers, which is disadvantageous to the toughness. The influence of the M-A constituents on the weld